Supplementary Information

Benefits of active site proximity in Cu@UiO-66 catalysts for efficient upgrading of ethanol to n-butanol

Jian Zhou[a,‡], Yaohui He[a,‡], Bing Xue[a], Yunhui Cheng[a], Danfeng Zhou[a], Dong Wang[a], Yajun He[a], Weixin Guan[a], Kegong Fang[b], Lijun Zhang[c], Jun Ni[a,*], and Xiaonian Li[a]

[a] *Institute of Industrial Catalysis, Zhejiang University of Technology, Hangzhou 310014, P.R. China*
[b] *State Key Laboratory of Coal Conversion, Institute of Coal Chemistry, Chinese Academy of Sciences, Taiyuan 030001, P.R. China*
[c] *Key Laboratory of Chemical Utilization of Forestry Biomass in Zhejiang Province, College of Science, Zhejiang A & F University, Hangzhou 311300, P.R. China*

***** Corresponding author and E-mail address: junni@zjut.edu.cn (Jun Ni)
‡ These authors contributed equally.

Table of Contents

Experimental Section

Materials

All chemicals were purchased from commercial sources and used without further purification. Specifically, zirconium chloride ($ZrCl_4$), anhydrous N,N-dimethylformamide (DMF), acetic acid (HAc), and copper acetylacetonate ($Cu(acac)_2$) were purchased from Aladdin, acetylacetonate ($C_5H_8O_2$) from Macklin, and 1,4-benzenedicarboxylic acid (H_2BDC) from Acros.

Synthesis of UiO-66 support

UiO-66 support was synthesized following the procedure reported in our previous work.[1] 5.25 g of $ZrCl_4$ and 3.71 g of H_2BDC were added to 256 mL of DMF at room temperature. Then, 38.4 mL of HAc and 2mL of water were added until all precursors were completely dissolved. The mixed solution was transferred to a hydrothermal vessel of 500 mL with Teflon liner and kept at 120 ºC for 24 h under static conditions. After cooling to room temperature, the resulting UiO-66 solid was collected via centrifugation and thoroughly washed with a mixture of methanol and DMF (v/v=1:4) three times, and methanol two times. Finally, the UiO-66 was dried under vacuum at 150 ºC for 12 h.

Synthesis of Cu@UiO-66 catalysts

Cu@UiO-66 catalysts were preparation via an impregnation-reaction method (IRM) adopted in our group.[1] The acetylacetone solution of $Cu(acac)_2$ was first prepared by dissolving 40.9, 81.8, 122.7, 204.5 mg of $Cu(acac)_2$ in 57.3 mL of acetylacetone, respectively. Then, 1.0 g of UiO-66 was added to the above solution and reacted at 50 ºC for 24 h before the acetylacetone solvent was slowly evaporated at 120 ºC. The remaining catalyst was further dried under vacuum overnight at 150 ºC to obtain the Cu@UiO-66 catalysts with the Cu weight loading of 1.0 %, 2.0 %, 3.0 %, and 5.0 %, respectively.

Synthesis of 2%Cu/UiO-66 catalyst

2%Cu/UiO-66 catalyst was prepared by an impregnation method: Briefly, 81.8 mg of $Cu(acac)_2$ was dissolved in 57.3 mL of acetylacetone solution. 1.0 g of UiO-66 was then added to the above solution. After drying in the air to evaporate acetylacetone, the catalyst was

obtained by further drying under vacuum at 150 ºC for 12 h.

Catalyst characterization

Textural properties of catalysts, namely BET surface area, pore volume, and pore diameter, were determined by N_2 adsorption-desorption using a Micromeritics 3FLEX apparatus with liquid nitrogen at the temperature of 77 K. The catalyst was outgassed at 150 ºC for 4h before analysis. X-ray diffraction (XRD) data were collected on an X'Pert PRO X-ray diffractometer between 2θ = 5º and 80º at 2º/min employing a Cu-Kα radiation source (λ =0.15406 nm). TEM imaging was performed on a Cu grid at an accelerating voltage of 200 kV using TALOS S-FEG TEM. The relative content of Cu was determined with the use of Wavelength-Dispersive XRF spectrometer (ThermoFisher Scientific, ADVANT'X 4200) and displayed in Table S1.

Table S1 The contents of Zr and Cu in Cu@UiO-66 catalysts.

Catalyst	The content of Zr (wt.%)		The content of Cu (wt.%)	
	XRF[a]	Calculated[b]	XRF[c]	Calculated[d]
1%Cu@UiO-66	92.66	32.61	3.37	1.19
2%Cu@UiO-66	89.66	32.23	6.51	2.34
3%Cu@UiO-66	86.88	31.90	9.11	3.34
5%Cu@UiO-66	83.37	31.26	14.08	5.28

[a] The content of Zr was measured by XRF.
[b] The content of Zr was calculated by taking the contents of C, H, and O into account.
[c] The content of Cu was measured by XRF.
[d] The content of Cu was calculated by taking the contents of C, H, and O into account.

Temperature-programed reduction (H_2-TPR) and Temperature-programed desorption of NH_3 and CO_2 (NH_3- and CO_2-TPD) experiments were performed on a homemade TPD apparatus. For H_2-TPR, 0.1g of catalyst was placed in a quartz reactor and heated from 50 ºC to 270 ºC at a rate of 5 ºC/min in a 10% H_2/Ar gas mixture (45 mL/min), and then maintained at 270 ºC for 0.5 h. A thermal conductivity detector (TCD) was used to record the amount of H_2 consumption during the reduction of catalysts. For NH_3- and CO_2-TPD, 0.1g of catalyst was heated from 30 ºC to 270 ºC at a rate of 10 ºC/min and reduced at 270 ºC for 4 h in a 10% H_2/Ar gas mixture (45 mL/min). After the reduction, the catalyst was cooled down to 50 ºC in Ar flow of 45 mL/min. At the same temperature, the NH_3 saturation uptake of the reduced catalyst was achieved by passing 10% NH_3/Ar (45 mL/min) for 0.5 h. After the NH_3 adsorption, the catalyst

was purged by Ar with a flow rate of 45 mL/min for 1 h. Finally, the temperature was linearly increased from 50 ºC to 300 ºC at a rate of 5 ºC/min and remained at 300 ºC for 1 h, while NH_3-TPD profiles were recorded with a TCD.

The surface area of metallic Cu ($S_{Cu}{}^0$) was determined by N_2O titration in the same home-built TPD apparatus, following the procedure described by Van Der Grift et al.[2, 3] Briefly, 0.1g of catalyst was reduced at 270 ºC for 0.5 h in a 10% H_2/Ar mixture at a flow rate of 45 mL/min. The corresponding hydrogen consumption detected by a thermal conductivity detector (TCD) was denoted as X. After cooling the catalyst to 100 ºC in Ar, a flow of 20% N_2O/N_2 (45 mL/min) was used to oxidize surface Cu atoms at 100 ºC for 0.5 h. The reactor was then flushed with Ar to remove the oxidant. Finally, another TPR experiment with the same procedure was initiated. The hydrogen consumption in the second TPR was denoted as Y. The surface area of metallic Cu was calculated as:

$$S_{Cu}{}^0 = 2 \times Y \times N_{av}/(X \times M_{Cu} \times 1.4 \times 10^{19}) = 1353 \times Y/X\ (m^2/g_{Cu})$$

where N_{av} is Avogadro's constant, M_{Cu} is the relative atomic mass of copper (63.46 g/mol), and 1.4×10^{19} is the number of Cu atoms per square meter, because the average surface area of Cu atom is assigned as 7.11×10^{-2} nm^2.

In situ FTIR (Fourier transform infrared spectroscopy) spectra were collected on a Nicolet IS50 FTIR spectrometer. 0.1g of catalyst was first mixed with 0.9g of KBr and ground into powder. 25 mg of the mixture was pressed into self-supporting wafers and mounted into an FTIR chamber. After being reduced by a 10% H_2/Ar gas mixture (45 mL/min) at 270 ºC for 4 h, the catalyst was cooled to 30 ºC and purged by Ar at a flow rate of 30 mL/min. Then, a background spectrum was collected as a reference before the introduction of pyridine. After the chamber was flushed with Ar (30 mL/min) for 0.5 h to remove any gas-phase and physically adsorbed pyridine, FT-IR spectra of pyridine adsorption over reduced Cu@UiO-66 catalysts were recorded and subtracted from the background spectrum.

Catalyst evaluation

All catalytic experiments were performed in a fixed-bed reactor. Typically, 0.5g of catalyst was placed in a tubular reactor (28 cm length, 8 mm internal diameter) and then reduced by a 10% H_2/N_2 gas mixture at 270 ºC for 4 h. The reaction was carried out under the following conditions: 270 ºC, 2 MPa, LHSV=4 mL/(h·g·cat), and N_2/ethanol(v/v)=500:1. Before admission of ethanol into the reaction system, ethanol was vaporized in a preheating section kept at 160 ºC. The total pressure of 2 MPa was achieved by regulating a back pressure valve after the reactor. The liquid products were condensed and analyzed by a Gas chromatograph (GC) with a flame ionization detector (FID) and an EN-20 column (30 m, 0.25 mm inner diameter, 0.25 μm film thickness).

The ethanol conversion, selectivity, and yield of products were calculated as follows：

$$\text{Ethanol conversion (\%)} = \frac{C\ mol\ of\ products}{C\ mol\ of\ (products + unreacted\ ethanol)} \times 100\%$$

$$\text{Product selectivity (\%)} = \frac{C\ mol\ of\ specific\ product}{C\ mol\ of\ products} \times 100\%$$

$$\text{Product yield (\%)} = \text{Ethanol conversion} \times \text{Product selectivity}$$

where C mol is the mole number of carbon in the products and unreacted ethanol.

The acetaldehyde condensation was carried out in a high-pressure reactor (50 mL). 0.05 g of catalysts and 20 mL of 10% acetaldehyde/toluene solution were then added. After the reaction time of 4 h at 250 ºC in N_2 with stirring speed at 800 rpm, the reactor was cooled down to room temperature and the samples were taken for analysis.

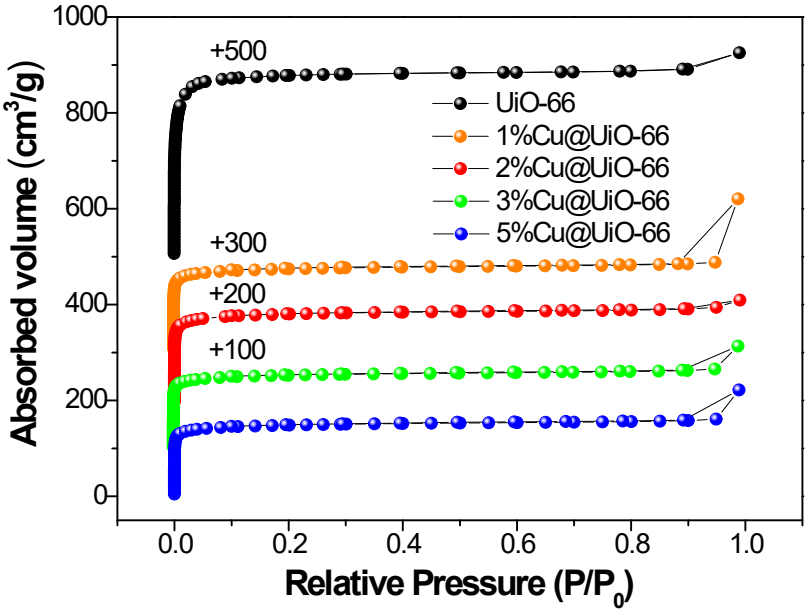

Fig. S1 N_2 adsorption-desorption of the UiO-66 support and Cu@UiO-66 catalysts.

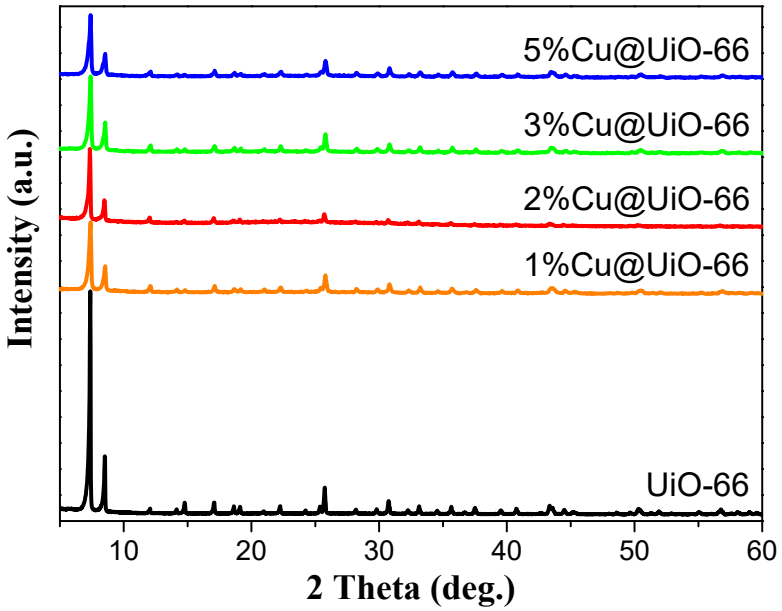

Fig. S2 XRD patterns of the UiO-66 support and reduced Cu@UiO-66 catalysts.

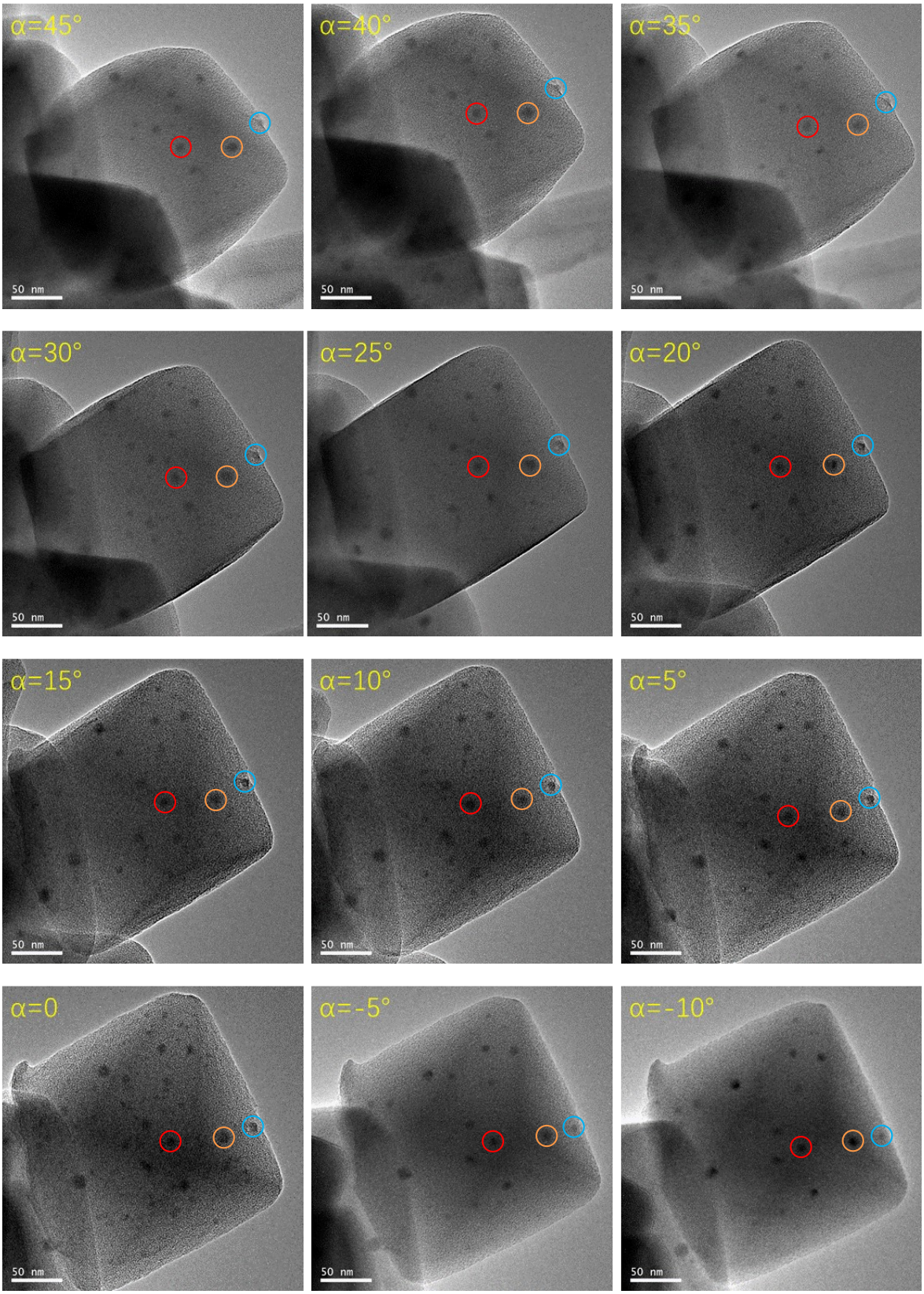
α=45°
α=40°
α=35°
α=30°
α=25°
α=20°
α=15°
α=10°
α=5°
α=0
α=-5°
α=-10°
50 nm

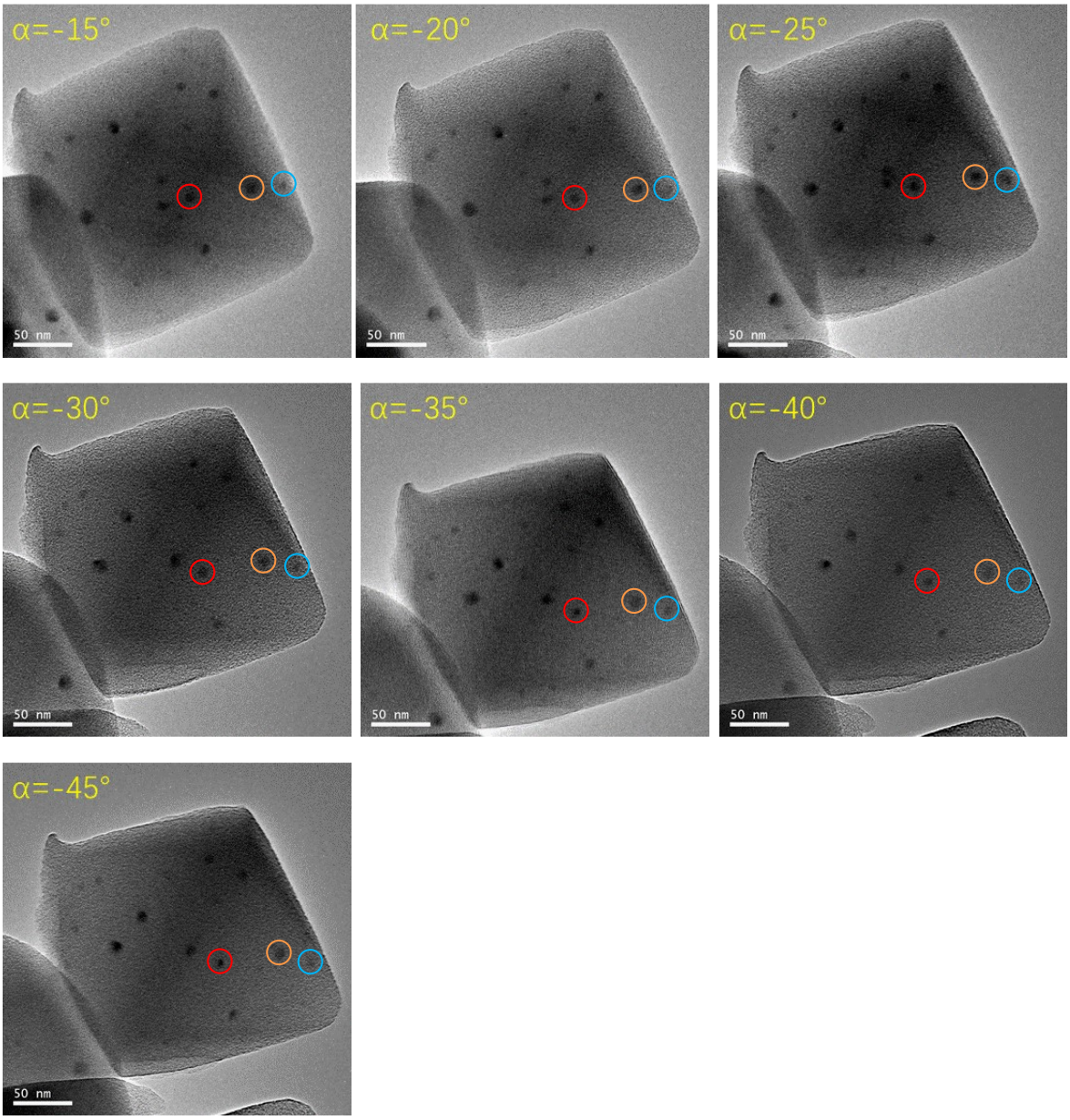

Fig. S3 TEM images of reduced 2% Cu@UiO-66 catalyst in the angle range from 45º to -45º.

Three representative Cu particles are circled. The one located on the external surface of UiO-66 is in a blue circle, the other two in the pores of UiO-66 are in red and orange circles. With the rotation of the catalyst from 45º to -45º, the one on the external surface of UiO-66 gradually moves away from the edge of the UiO-66 framework and its signal intensity also varies. In contrast, there is no significant movement and signal intensity change of the Cu particles in the pores of UiO-66.

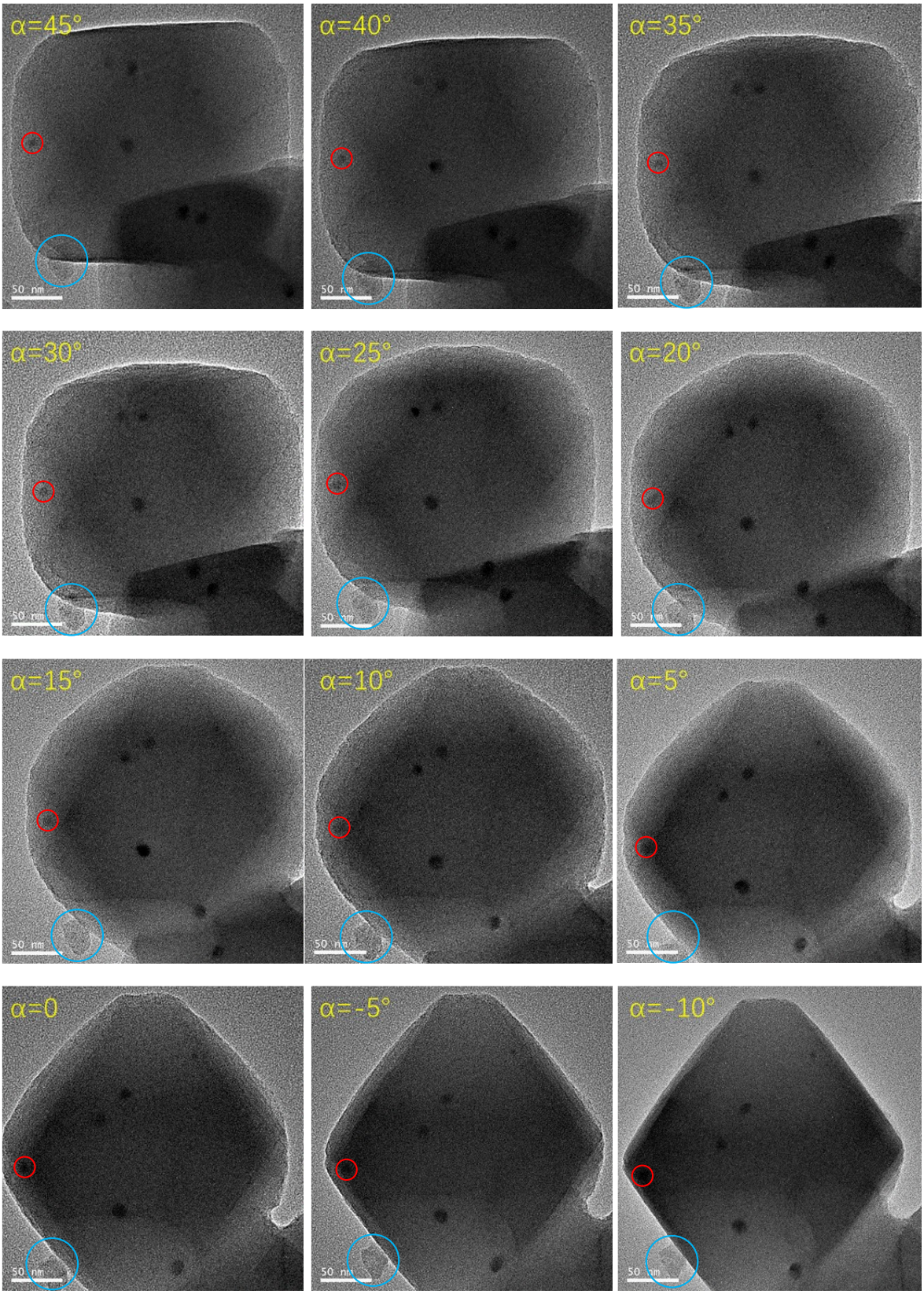
α=45°
α=40°
α=35°
α=30°
α=25°
α=20°
α=15°
α=10°
α=5°
α=0
α=-5°
α=-10°
50 nm

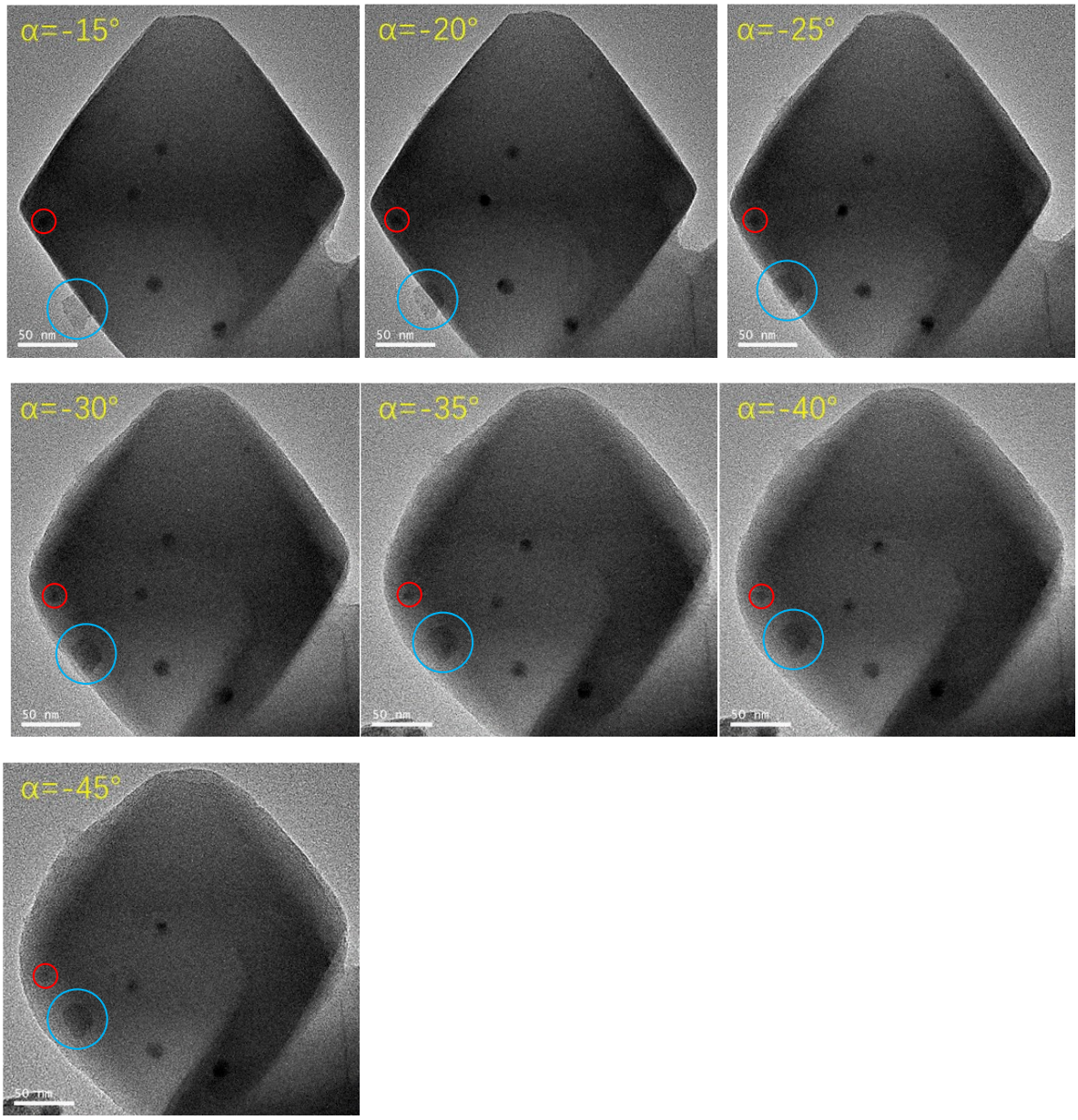

Fig. S4 TEM images of spent 2% Cu@UiO-66 catalyst in the angle range from 45º to -45º.

A representative Cu particle is circled in red and the amorphous carbon produced during the reaction is circled in blue. With the rotation of the catalyst from 45º to -45º, the amorphous carbon turns from the front to the back of UiO-66. In contrast, the Cu particle remains in the framework of UiO-66 regardless of the rotation angle. This is strong evidence that this Cu particle is in the pores of UiO-66.

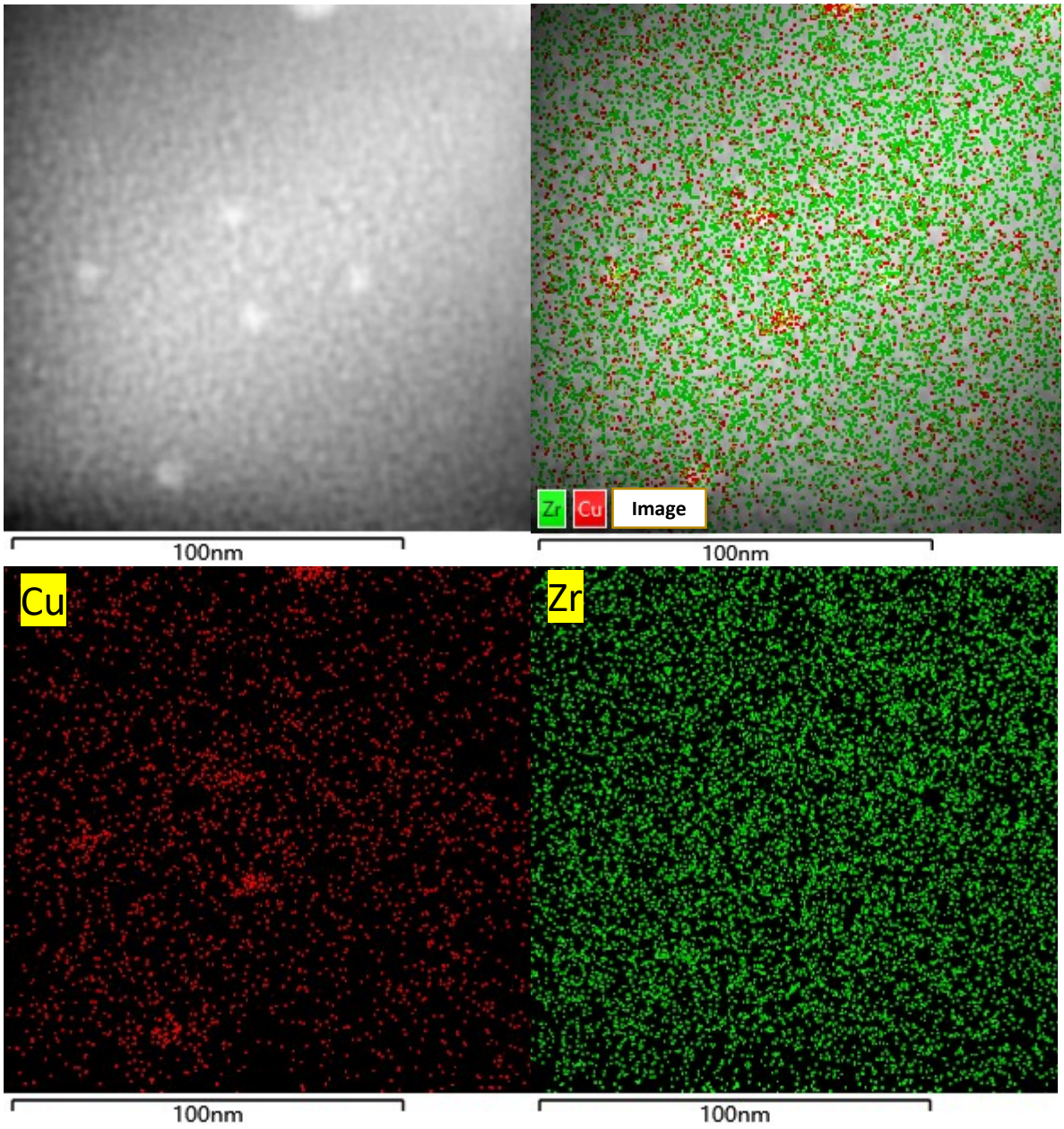

Fig. S5 EDS mapping of reduced 2% Cu@UiO-66 catalyst.

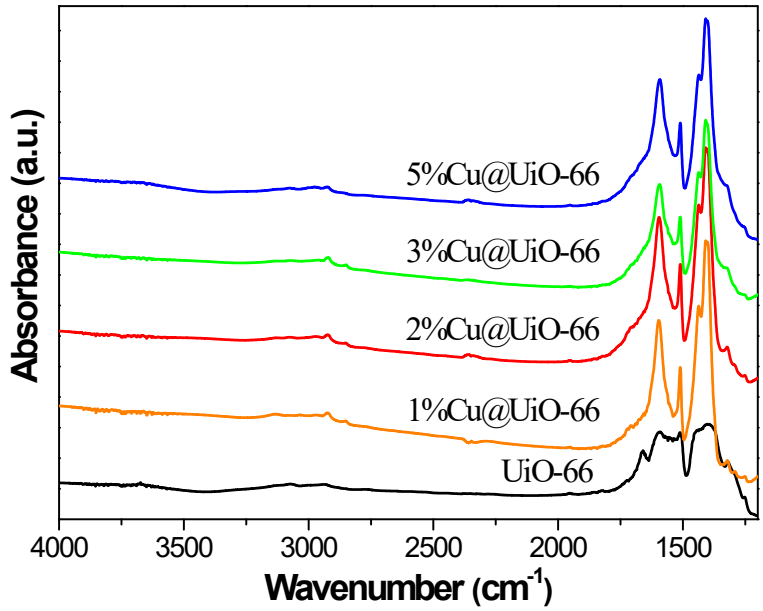

Fig. S6 *In situ* FTIR spectra of the reduced UiO-66 support and reduced Cu@UiO-66 catalysts.

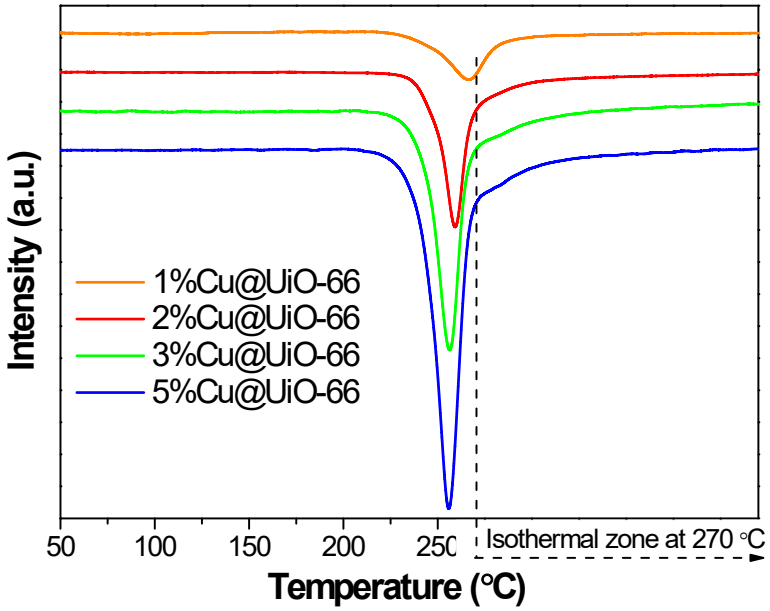

Fig. S7 H_2-TPR profiles of Cu@UiO-66 catalysts.

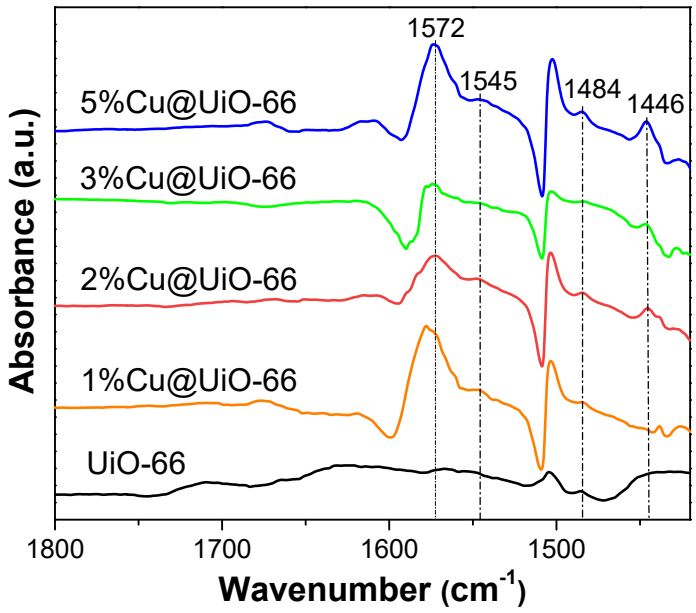

Fig. S8 *In situ* FTIR of pyridine adsorption on the reduced UiO-66 support and reduced Cu@UiO-66 catalysts.

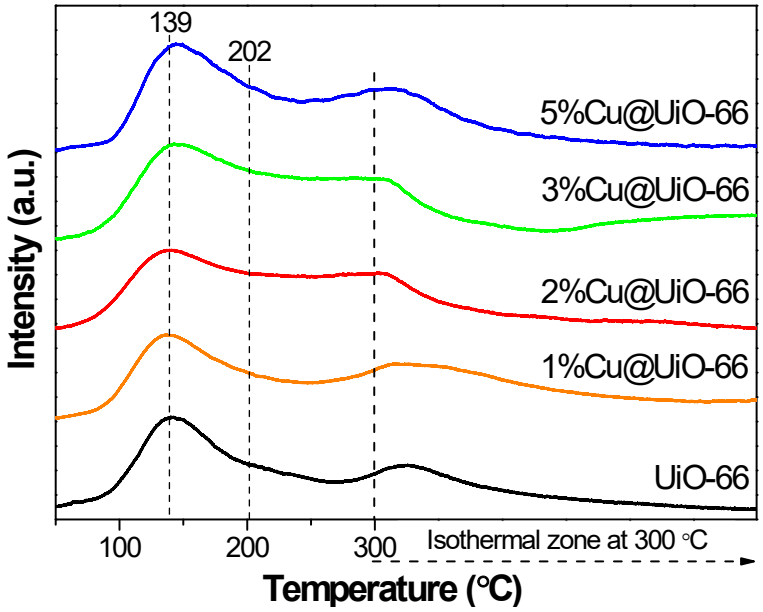

Fig. S9 NH_3-TPD on the reduced UiO-66 support and reduced Cu@UiO-66 catalysts.

The peak in the isothermal zone at 300 ºC is related to the loss of acetate due to the introduction of acetic acid as modulator molecules in the synthesis of UiO-66 and thus was not taken into account.[4]

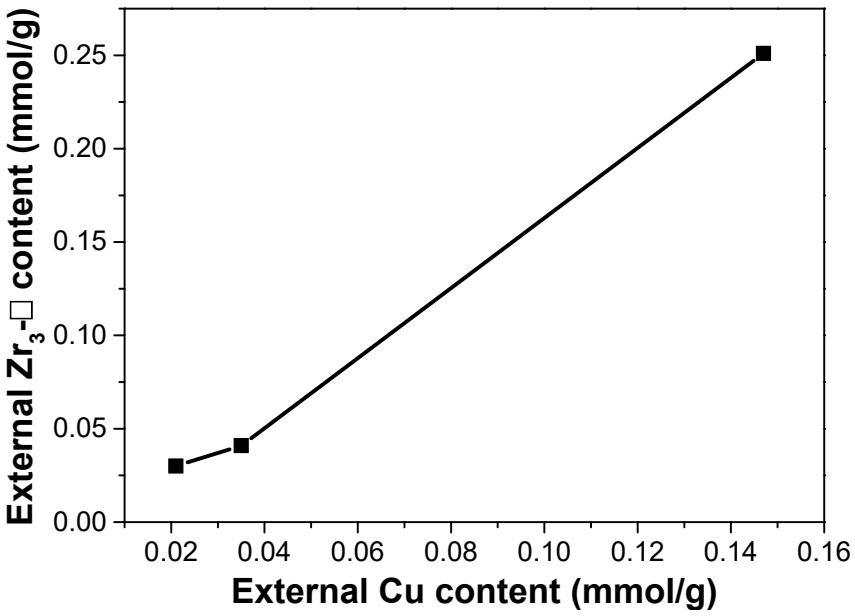

Fig. S10 The correlation between external Cu content and Zr_3-□ content.

Table S2 The Zr_3-□ content of Cu@UiO-66 catalysts.

Catalyst	Zr_3-□ content (mmol/g)			
	Internal[a]	Via dehydroxylation[b]	External[c]	Total[d]
1%Cu@UiO-66	0.046	0.370	0.030	0.446
2%Cu@UiO-66	0.090	0.326	0.041	0.457
3%Cu@UiO-66	0.091	0.325	0.251	0.667
5%Cu@UiO-66	0.092	0.324	0.263	0.679

[a] Generated in Scheme 2b and calculated according to the hydrogen consumption of the reduction of Cu on the internal surface of UiO-66.

[b] Generated in Scheme 2c and calculated according to the difference between the total content of Zr_3-□ and the contents of Zr_3-□ generated both in Scheme 2b and Scheme 2d.

[c] Generated in Scheme 2d and calculated according to the difference between the total content of Zr_3-□ and that generated on UiO-66 in Scheme 2c as listed in Table 3.

[d] Calculated to be the same amount as that of 6-fold coordinated Zr sites determined by NH_3-TPD in Table 3.

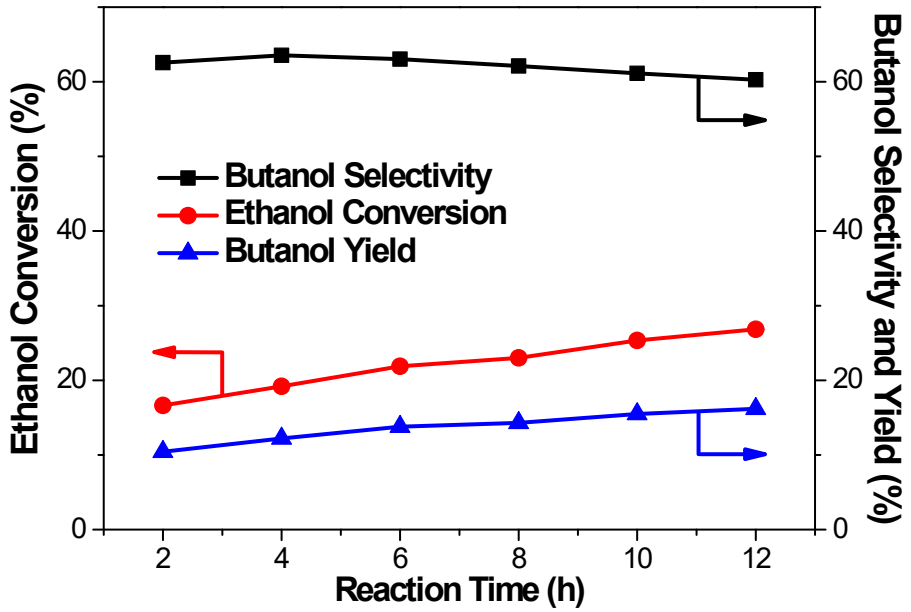

Fig. S11 The catalytic performance of 1%Cu@UiO-66 catalyst with time on-stream.

Table S3 The activity of catalysts in the reaction steps of the Guerbet route.

Catalyst	The activity of catalysts (%)				
	Dehydrogenation[a]	Dehydration[b]	Condensation[c]	Hydrogenation[d]	Liquid yield[e]
1%Cu@UiO-66	23.5	0.29	19.0	19.0	98.3
2%Cu@UiO-66	26.5	0.34	21.9	21.9	98.2
3%Cu@UiO-66	28.2	0.36	22.7	22.7	97.4
5%Cu@UiO-66	28.0	0.29	22.8	22.8	98.4
2%Cu@UiO-66[f]	42.7	0.24	34.5	34.5	92.5
2%Cu/UiO-66[g]	19.5	0.08	15.7	15.7	98.7

[a] Dehydrogenation ability includes the yields of ethanol derivatives except for diethyl ether.

[b] Dehydration ability includes the yield of diethyl ether.

[c] Condensation ability includes the yields of butyraldehyde, butanol, C_6 products, and others. All of them are derived from acetaldehyde condensation.

[d] Hydrogenation ability includes the yields of butyraldehyde, butanol, C_6 products, and others.

[e] The mass ratio of liquid products in the output to reactants in the input.

[f] The reaction temperature was 280 ºC.

[g] The catalyst was synthesized by an impregnation method using acetylacetone as the solvent.

Table S4 Catalytic performance of Cu@UiO-66 catalysts at 280 ºC.[a]

Catalyst	Conv. (%)	Selectivity[b] (%)							BuOH Yield (%)
		AcH	Ether	EA	BuH	BuOH	C_6 products	Others	
1%Cu@UiO-66	38.9	7.9	0.7	8.1	5.6	52.8	15.9	6.1	20.5
2%Cu@UiO-66	42.9	7.7	0.5	11.5	5.7	50.3	17.9	6.4	21.6
3%Cu@UiO-66	46.6	6.9	0.8	12.5	6.3	46.5	20.5	6.5	21.7
5%Cu@UiO-66	50.7	5.3	0.5	17.7	5.1	43.9	24.2	3.3	22.2

[a] Conversion, selectivity and yield were obtained at steady-state; reaction conditions: 0.5 g catalyst, 280 ºC, 2 MPa, LHSV=2 h^{-1}, N_2/ethanol(v/v) = 500:1.

[b] AcH = acetaldehyde; Ether = diethyl ether; EA= ethyl acetate; BuH = butyraldehyde; BuOH = butanol; C_6 products mainly include 2-ethylbutyraldehyde, hexaldehyde, 2-ethylbutanol, and 1-hexanol; Other products include 2-pentanone, 1,1-diethoxyethane, butyl acetate, etc.

Table S5 Catalytic performance of 2%Cu@UiO-66 catalyst at various residence times.[a]

LHSV (h^{-1})	Conv. (%)	Selectivity[b] (%)							BuOH Yield (%)
		AcH	Ether	EA	BuH	BuOH	C_6 products	Others	
1	27.3	8.1	0.8	9.7	4.1	60.5	9.2	7.4	16.5
2	26.8	9.0	1.2	8.3	4.3	60.3	8.2	8.7	16.2
4	22.6	11.5	1.3	8.2	5.5	56.5	7.6	9.4	12.8

[a] Conversion, selectivity, and yield were obtained at steady-state; reaction conditions: 0.5 g catalyst, 250 ºC, 2 MPa.

[b] AcH = acetaldehyde; Ether = diethyl ether; EA= ethyl acetate; BuH = butyraldehyde; BuOH = butanol; C_6 products mainly include 2-ethylbutyraldehyde, hexaldehyde, 2-ethylbutanol, and 1-hexanol; Other products include 2-pentanone, 1,1-diethoxyethane, butyl acetate, etc.

Table S6 Catalytic performances reported for Cu-based catalysts.

Catalyst	Reactor	Reaction Conditions	Conversion (%)	BuOH Selectivity (%)	BuOH Yield (%)	Ref.
Cu@UiO-66	**Fixed-bed**	**280 ºC, 2 MPa, LHSV=4 mL/(h·g·cat)**	**50.7**	**43.9**	**22.2**	**This work**
Cu/Al_2O_3	Fixed-bed	260 ºC, 10 MPa, LHSV=1.97 h^{-1}, sc CO_2	48	7	3	5
Cu/ZSM-5	Fixed-bed	260 ºC, 10 MPa, LHSV=1.97 h^{-1}, sc CO_2	15	2	0	5
Cu/CeO_2	Fixed-bed	260 ºC, 10 MPa, LHSV=1.97 h^{-1}, sc CO_2	39	35	13	5
$Cu/HSA\text{-}CeO_2$	Fixed-bed	260 ºC, 10 MPa, LHSV=1.97 h^{-1}, sc CO_2	67	45	30	5
Cu/TiO_2	Fixed-bed	260 ºC, 10 MPa, LHSV=1.97 h^{-1}, sc CO_2	53	25	13	5
$Cu/SiO_2\text{-}Al_2O_3$	Fixed-bed	260 ºC, 10 MPa, LHSV=1.97 h^{-1}, sc CO_2	30	14	6	5
$Cu\text{-}CeO_2/AC$	Fixed-bed	250 ºC, 2MPa, LHSV=4 mL/(h·g·cat), 48h	46.2	41.3	19.1	6
$G_x\text{-}CuCeO_2/AC$	Fixed-bed	250 ºC, 2 MPa, LHSV=2h^{-1}	42.3	48.9	20.7	7
Cu/HSAG	Fixed-bed	230 ºC, 5MPa, LHSV=2.4 mL/(h·g·cat)	17	4	0.7	8
2.5Cu2.5Ni/HSAG	Fixed-bed	230 ºC, 5MPa, LHSV=2.4 mL/(h·g·cat)	20	4	0.8	8
5Cu-Mn/HSAG	Fixed-bed	230 ºC, 5MPa, LHSV=2.4 mL/(h·g·cat)	27	33	8.9	8
2.5Cu2.5Ni-Mn/HSAG	Fixed-bed	230 ºC, 5MPa, LHSV=2.4 mL/(h·g·cat)	37	36	13.3	8
5Cu/G	Fixed-bed	230 ºC, 5MPa, LHSV=2.4 mL/(h·g·cat), 24h	17	4	0.7	9
5Cu-Mg/G	Fixed-bed	230 ºC, 5MPa, LHSV=2.4 mL/(h·g·cat), 24h	26	26	6.8	9
5Cu-Ba/G	Fixed-bed	230 ºC, 5MPa, LHSV=2.4 mL/(h·g·cat), 24h	28	13	3.6	9
5Cu-Zn/G	Fixed-bed	230 ºC, 5MPa, LHSV=2.4 mL/(h·g·cat), 24h	25	11	2.8	9
5Cu-Mn/G	Fixed-bed	230 ºC, 5MPa, LHSV=2.4 mL/(h·g·cat), 24h	27	33	8.9	9
Cu/HT	Parr autoclave	215 ºC, 4MPa	24.7	53	13.1	10
$0.5\%Cu/Al_2O_3$	Parr autoclave	275 ºC, 3h	25.0	78.8	19.7	11
$1\%Cu/Al_2O_3$	Parr autoclave	275 ºC, 3h	27.2	78.5	21.4	11
$2\%Cu/Al_2O_3$	Parr autoclave	275 ºC, 3h	31.5	81.9	25.8	11
$5\%Cu/Al_2O_3$	Parr autoclave	275 ºC, 3h	33.5	80.2	26.9	11

10%Cu/Al_2O_3	Parr autoclave	275 ºC, 3h	27.2	71.9	19.6	11

Table S7 The activity of acetaldehyde condensation over Cu@UiO-66 catalysts.[a]

Catalyst	Conversion (%)	Crotonaldehyde Selectivity (%)	Crotonaldehyde Yield (%)
UiO-66	40.4	100	40.4
1wt%Cu@UiO-66	52.6	100	52.6
2wt%Cu@UiO-66	56.0	100	56.0
3wt%Cu@UiO-66	57.9	100	57.9
5wt%Cu@UiO-66	59.9	100	59.9

[a] Conversion, selectivity and yield were obtained at steady-state; reaction conditions: 0.05 g catalyst, 250 ºC , 20 mL of 10% acetaldehyde/toluene solution.

Please noted that external Zr_3-□ may participate in the condensation when using acetaldehyde as the reactant, thus the conversion of acetaldehyde increases as the increase in Cu loading.

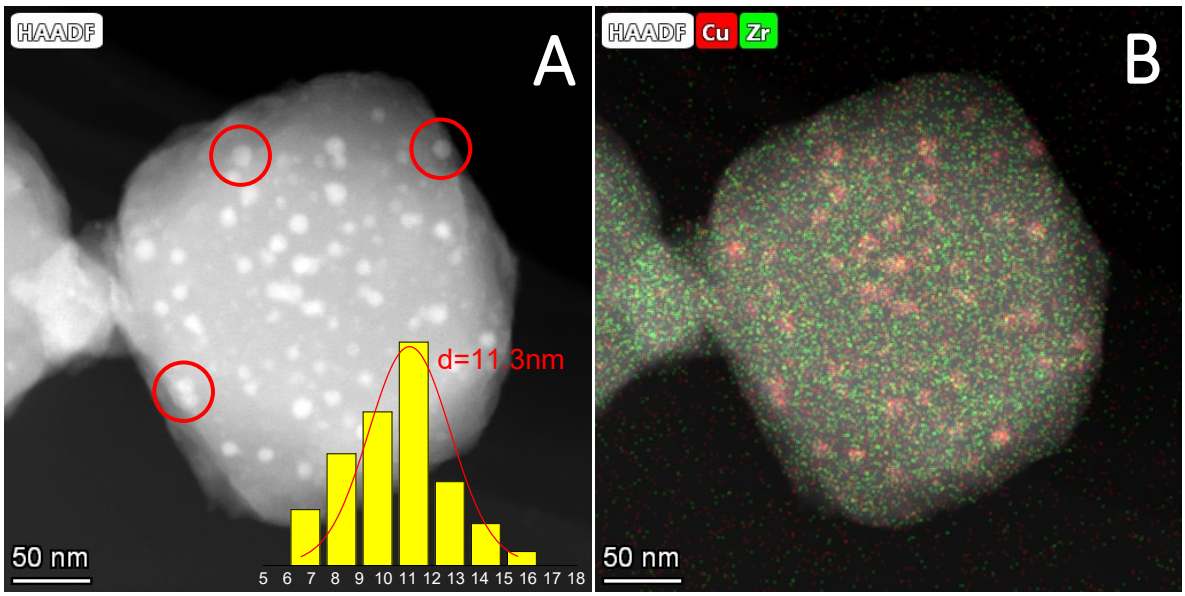

Fig. S12 (A) TEM image and corresponding histogram, and (B) EDS mapping of reduced 2%Cu/UiO-66 catalyst.

Comparing with the 2%Cu@UiO-66 catalyst, the 2%Cu/UiO-66 catalyst has more Cu particles located at the edge of UiO-66 support and has an average Cu particle size of 11.26 nm. Moreover, the surface area of metallic Cu per gram of Cu (S_{Cu}^{0}) is only 112.4 m^2/g_{Cu}, much less than that of 2%Cu@UiO-66 (301.5 m^2/g_{Cu}), meaning a severe Cu aggregation. This larger particle size of Cu on the 2%Cu/UiO-66 catalyst indicates that the interaction between Cu metals and Zr_3-□ is weaker than that on the 2%Cu@UiO-66 catalyst. Although some Cu metals are interacting with Zr_3-□, their number is significantly reduced, thus the activity in terms of dehydrogenation, dehydration, condensation, and hydrogenation reduces.

References

1. D. Jiang, G. Fang, Y. Tong, X. Wu, Y. Wang, D. Hong, W. Leng, Z. Liang, P. Tu, L. Liu, K. Xu, J. Ni and X. Li, *ACS Catal.*, 2018, 8, 11973-11978.
2. C. J. G. Van Der Grift, A. F. H. Wielers, B. P. J. Jogh, J. Van Beunum, M. De Boer, M. Versluijs-Helder and J. W. Geus, *J. Catal.*, 1991, 131, 178-189.
3. S. Xia, R. Nie, X. Lu, L. Wang, P. Chen and Z. Hou, *J. Catal.*, 2012, 296, 1-11.
4. G. C. Shearer, S. Chavan, S. Bordiga, S. Svelle, U. Olsbye and K. P. Lillerud, *Chem. Mater.*, 2016, 28, 3749-3761.
5. J. H. Earley, R. A. Bourne, M. J. Watson and M. Poliakoff, *Green Chem.*, 2015, 17, 3018-3025.
6. D. Jiang, X. Wu, J. Mao, J. Ni and X. Li, *Chem. Commun.*, 2016, 52, 13749-13752.
7. Y. Tong, J. Zhou, Y. He, P. Tu, B. Xue, Y. Cheng, J. Cen, Y. Zheng, J. Ni and X. Li, *ChemistrySelect*, 2020, 5, 7714-7719.
8. C. Lopez-Olmos, A. Guerrero-Ruiz and I. Rodríguez-Ramos, *Catal. Today*, 2020, 357, 132-142.
9. C. Lopez-Olmos, M. V. Morales, A. Guerrero-Ruiz and I. Rodríguez-Ramos, *Ind. Eng. Chem. Res.*, 2020, 59, 16626-16636.
10. P. Benito, A. Vaccari, C. Antonetti, D. Licursi, N. Schiarioli, E. Rodriguez-Castellón and A. M. Raspolli Galletti, *J. Clean. Prod.*, 2019, 209, 1614-1623.
11. A. V. Chistyakov, S. A. Nikolaev, P. A. Zharova, M. V. Tsodikov and F. Manenti, *Energy*, 2019, 166, 569-576.